Journal of Solid Mechanics Vol. 10, No. 1 (2018) pp. 86-97

# Influence of Notch Depth-to-Width Ratios on *J*-Integral and Critical Failure Load of Single-Edge Notched Tensile Aluminium 8011 Alloy Specimens

C. S. Sumesh [*], P. J. Arun Narayanan

*Department of Mechanical Engineering, Amrita School of Engineering, Coimbatore Amrita Vishwa Vidyapeetham, India*

Received 19 September 2017; accepted 13 December 2017

**ABSTRACT**

In this paper, the influence of notch depth-to-width ratios on *J*-integral and critical load of Aluminium 8011 alloy specimens with *U*-notch under Mode I loading are studied. Using experiments, for a set of specimens having different notch depth–to–width ratios, *J*-integral was found and the same was verified using analytical methods. Further, using the results obtained from the experiments, failure assessment diagrams (FAD) were plotted for the same ratios, to determine the safe or critical load and the type of failure mechanism was also studied. The results show that, for both shallow and deep notch depths, the *J*-integral values obtained from the experimental method, are in very close agreement with the analytical values. *J*-integral values decrease with increase in notch depth and increase with increase in applied load. Furthermore, from FAD, the safe load decreases when the notch depth-to-width ratio increases and it was found that, all the tested specimens failed due to elastic plastic deformation mechanism.


**Keywords:** Aluminium 8011 alloy; Notch depth; *J*-integral; Fracture toughness; Critical failure load.

## 1 INTRODUCTION

SHEET metal forming is a vital manufacturing process used in the automobile, aerospace, agriculture and architecture industries. In the present paper we have considered Aluminium 8011 alloy to make the specimens. Aluminium alloy 8011 in sheet form has found widespread application in construction industries and automobile as a result of their good physical and chemical properties such as formability, corrosion, and light weight. The significance of failure assessment or life prediction of structures is increasing day by day. The applicability of a material in a particular application depends up on its structural integrity. Flaws in the structure are generally not encouraged for critical applications in aerospace and automotive sectors, but still based up on the conditions governing the system, even a structure with flaw can be used. Behaviour of a crack under loading is the main concept behind fracture mechanics. Fracture mechanics basically uses the concepts of either Linear Elastic Fracture Mechanics (LEFM) or Elastic Plastic Fracture Mechanics (EPFM). LEFM assumes elastic behaviour of materials under loading. EPFM deals with materials which are generally ductile. They show a considerable area of

[*] Corresponding author.
*E-mail address: cs_sumesh@cb.amrita.edu* (C.S.Sumesh).

elastic deformation and large area of plastic deformation. EPFM is studied using parameters like Crack Tip Opening Displacement (CTOD), *J*-Integral etc. *J*-Integral gives the change in potential energy when the crack propagates.The *J*-integral is a line integral (path-independent) around the crack tip. Predicting the failure of structures with defect is of great significance and the methods to predict failure of material with defect are also available. In this paper, *J*- integral is calculated using experimental method and it is validated using analytical techniques.

Experiments are carried out on Al 7075-T6 and Electroless Nickel deposits coated Al 7075-T6 to study the Fracture Toughness and found that coating gave a significant improvement in the fracture behaviour (performance) of the substrate [1]. *J*-integral and crack opening displacements for centre cracked strip under tension and edge cracked strip subjected to bending have been studied. They assumed plane stress conditions and used Ramberg Osgood equations [2]. Vijayan et al., [3], have studied the mechanical strength and properties of carbon nanotube (CNT) reinforced foamed poly ether ketone (PEK) and found that tensile strength of CNT reinforced foamed PEK was relatively higher than unfilled PEK. Kumar et al., [4], have proposed equations to find *J*-integral under fully plastic and elastic plastic conditions. J-integral with a cyclic stress – strain curve under monotonic loading have studied by Shimakawa et al., [5]. These results are verified by experimental methods. Rice [6], has established a method to study the effect of parameters including stress intensity, plastic zone size, and crack tip opening displacement on the path dependent integral around the crack tip under plain strain conditions. The relation between caustic diameter and *J*-integral of the specimen under three point bend loading in steel using experimental method have studied by Alan Zehnder et al., [7]. Begley and Landes [8], suggested an experimental method to find *J*-integral. Besides, Montgomery [9], has discussed guidelines to be followed in finding the *J*-integral of AISI 304 Stainless Steel with different geometry and size under tension and compression. Aldo Frediani [10], has studied *J*-integral experimentally by assuming plane stress conditions.

The effect of notch on limit load for two different steels at different temperatures have studied by Madrazo et al., [11]. Another main work related to FAD is found in the work, done by Tipple and Thorwald [12], which is very much related to the work done in this paper. This is later applied in FAD to analyze the structural stability. Akhurst and Milne [13], derive experimentally the FAD for austenitic steel specimens of different geometries. This in fact is further used to test the accuracy of different failure assessing theories. Failure assessment diagrams have also been used in the work by Hasanaj et al., [14], to analyze defects in pipelines. The defects studied include failure due to plastic collapse and also elastic plastic failure. A probability of defects occurrence is also calculated. Structural integrity analysis has also made use of Failure assessment diagram as seen in Bergant et al., [15]. The integrity of steam generator tubes are assessed in this paper as such predicting the failure modes and lodes of tubes which have flaws. The concept of *J*-*R* curve has been applied for this purpose. Cases of cracks with shapes like semi elliptical on surfaces in circular hollow sections of *X* and *K* joints have been assessed for failure using FAD as in Qian [16]. The studies include the material and geometric dependence of the curves in FAD. The dependence of the curve on crack-front location, crack depth ratio, crack aspect ratios is observed. A parametric expression is found to be derived. The integrity of a structure based on the notch, *U* or *V*, is studied in Matvienko [17], where a notch is considered to be as a crack. The FAD are derived hence and the fracture toughness by load separation method. An acceptable notch is determined. In the paper by Matvienko [18], deals with deriving safety factors against fracture for structural integrity. The safety factors are calculated and then applied in failure assessment diagrams for analyzing the integrity of notched specimens. Failure assessment diagrams have also been derived in Elasaadany et al., [19], along with shake down boundary in cracked pipe bends. As usual FAD is obtained using the *J*-integral parameter with shake down limit moments. The maximum load is calculated along with the elastic domain. Similar to the concept of the common FAD, a strain based FAD (SB-FAD) is derived for the same purpose of predicting failure as in the work of Horn et al., [20] for sharp defects. Here curved wide plates with notches that are shallow are tested both experimentally and numerically. A modified SB-FAD is also derived for non-sharp defects and compared. Assessment of failure under different conditions without FAD is seen to be done in Parise et al., [21]. Here pipes with surface cracks subjected to reeling are assessed for which a strain based expression is derived. FEM methodology is used to validate the result. A condition of components subjected to rolling contact loading is also assessed for safety using the failure assessment diagram methodology as seen in Donzella and Petrogalli [22]. The FAD provided different areas of ruptures and the safe area is indicated. Another application of FAD is mentioned in Lie and Li [23] to predict the failure pressures of cracked metal cylinders. Different levels of FADs are derived and are compared for conservatism. Each level of FAD is derived using different methods. And a regression equation is derived based on the last level FAD found for failure prediction.

From the above literature review, no similar work has been done on this material. In this paper, *J*-integral was found experimentally for different notch depth to width ratios and the same was validated using analytical methods. Using the results obtained from *J*-integral calculations, failure assessment diagrams (FAD) were plotted for

specimens having same notch depth to width ratios, in order to determine the safe load that can be applied on the material without failure and the mechanism by which the material will fail was also studied. The detailed description of experimental procedure is explained.

## 2 METHODOLOGY

### *2.1 Experimental procedure*

The specimens used for the experiments were made from Aluminium alloy 8011. The % composition of the alloy is given in Table 1. Before conducting the experiment, six specimens of dimensions, width 22 *mm*, and length 88 *mm* were made from a large plate of 2 *mm* thickness as per ASTM E1820 standard. A notch of 1 *mm* width was machined on one side of the specimens. A pre crack from the notch tip was introduced by cyclic loading. The depth of the notch in each specimen was 5.5 *mm*, 8.25 *mm*, 11 *mm*, 13.75 *mm*, 16.5 *mm* and 19.25 *mm* respectively. In these, notch depths 5.5 *mm*, 8.25 *mm*, and 11 *mm* are considered as Shallow notch depths and 13.75 *mm*, 16.5 *mm* and 19.25 *mm* are considered as Deep notch depths. Then each specimen was loaded on to the UTM (Model: H25KT, Capacity 2500 *kg*) as shown in Fig. 1(a). Fig. 1(b) shows the specimen used in this study, as per ASTM E1820 standard and all dimensions are in *mm*. Further, using the UTM a monotonic load was applied gradually on the specimen till it failed.

From the uniaxial tensile testing, the load vs. load line displacement curve for the six specimens is plotted as shown in Fig. 2. In the diagram, the region where the load varies from zero to the ultimate load, is considered for the study. For detailed study, this region is further split into two; from zero to yield point and from yield point to ultimate. From the Load – load line displacement data obtained from uniaxial testing, a set of six load line displacement (Δ) values were obtained in the range zero to yield point at equal intervals. The values of Δ obtained in that range, for shallow notched depth specimens are, 0.00, 0.221, 0.442, 0.663, 0.884, and 1.105 *mm*. Also, the equal interval six values of Δ in the range yield point to ultimate, for shallow notched depth specimens are, 1.150, 1.199, 1.248, 1.297, 1.346, and 1.396 *mm*. Then, area under the load vs. load line displacement curve for these values was found using the trapezoidal rule, for each notch depth. These values gave the strain energy released (*U*), during the notch expansion.

Further, *U* vs. notch depths for the selected values of load line displacements for the two regions are plotted, as shown in Fig. 3(a) and (b). Using curve fitting method available in MATLAB, equation of each curve is obtained and slope of the tangent at each (Δ) values was found. From the slope values, the *J*-integral was calculated using the equation given in Eq. (1).

$$J = \frac{-1}{B}\left(\frac{\partial U}{\partial a}\right)_{\Delta} \tag{1}$$

Similarly, for deep notched specimens, the Δ values in the region from zero to yield point are, 0.000, 0.096, 0.192, 0.288, 0.384, and 0.480 *mm* and the values in the range yield to ultimate point are, 0.784, 0.806, 0.827, 0.848, 0.870, and 0.892 *mm*. Same procedure was repeated and *J*-integral values were calculated using Eq. (1). Figs. 4(a) and (b), shows the variation of *U* vs. notch depths for the selected values of load line displacements for the two regions.

**Table 1**
Percentage composition of constituents in Aluminium 8011 alloy.

| Element | Al | Cr | Cu | Fe | Mg | Mn | Si | Ti | Zn |
|---|---|---|---|---|---|---|---|---|---|
| % | 97.3 – 98.9 | 0.05 | 0.10 | 0.6 – 1.0 | 0.05 | 0.20 | 0.5 – 0.90 | 0.08 | 0.10 |

### *2.2 Analytical procedure*

In 1943, Ramberg and Osgood proposed a well-known formula,

$$\frac{\varepsilon}{\varepsilon_0} = \frac{\sigma}{\sigma_0} + \alpha\left(\frac{\sigma}{\sigma_0}\right)^n \tag{2}$$

To describe a non-linear relationship between stress and strain in materials nearer to their yield point, when subjected to uniaxial loading starting from zero. Ramberg Osgood constants were obtained from Al 8011 alloy specimen material's log – log true stress – plastic strain curve, and the same was calculated from the engineering stress – strain curve. A specimen was made from Al 8011 alloy as per ASTM B557-06 standard, all dimensions are in mm, as shown in Fig. 5.

The specimen is loaded on to UTM (Model: H25KT, Capacity 2500 *kg*) and subjected to a uniaxial tensile test. The engineering stress – strain curve obtained from the uniaxial tensile test is shown in Fig. 6 below. Using the following equations, true stress and true strain are calculated from the engineering stress – strain values.

$$\varepsilon_T = \ln\left(\varepsilon_E + 1\right) \tag{3}$$

$$\sigma_T = \sigma_E \left(\varepsilon_E + 1\right) \tag{4}$$

Then using the log-log true stress – plastic strain curve, as shown in Fig.7, the Ramberg Osgood constants are determined from the slope and y-intercept as $n$ =16 and $\alpha$ =3.097.

### *2.3 J-integral calculations*

The following equations were used to find elastic and plastic *J*-integrals and the total *J*-integral of Single Edge Notched Tension (SENT) specimens for different notch to depth ratios.

$$J_{total} = J_{elastic} + J_{plastic} \tag{5}$$

where

$$J_{elastic} = \frac{K_I^2}{E} = \frac{P^2 f^2\left(a/W\right)}{B^2 W E} \tag{6}$$

where

$$f\left(a/W\right) = \frac{\sqrt{2\tan\left(\frac{\pi a}{2W}\right)}}{\cos\left(\frac{\pi a}{2W}\right)}\left[0.752 + 2.02\left(\frac{a}{W}\right) + 0.37\left(1 - \sin\left(\frac{\pi a}{2W}\right)\right)^3\right] \tag{7}$$

$$J_{plastic} = \alpha\varepsilon_0\sigma_0 b h_1\left(a/W, n\right)\left(\frac{P}{P_0}\right)^{n+1} \tag{8}$$

$$P_0 = 1.072\eta B b \sigma_0 \tag{9}$$

$$\eta = \sqrt{1 + \left(\frac{a}{b}\right)^2} - \left(\frac{a}{b}\right) \tag{10}$$

$\sigma_0$ is taken as the yield strength of the material, which can be obtained from the previous tensile test data. From the above relations, we can understand that $J_{elastic}$ is dependent on the load P applied on the specimen, depth of notch, width and thickness of the specimen and Modulus of elasticity. Whereas $J_{plastic}$ is dependent on additional factors like load at yielding, unnotched length and strain hardening exponent. In this present work, six specimens of different notch depths, 5.5 *mm*, 8.25 *mm*, 11 *mm*, 13.75 *mm*, 16.5 *mm* and 19.25 *mm* are considered. In the

calculations, we assumed plane stress conditions and width and thickness of specimen are fixed as 22 *mm* and 2 *mm* respectively and using the above Eqs. (5)- (10), the total *J*-integral was calculated for the six cases. The values of applied force, *P*, are taken from the Fig.2, corresponding to the selected Δ values.


(a)

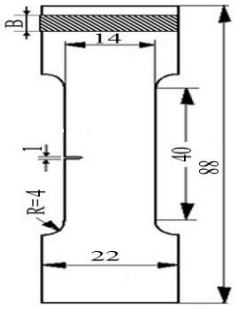


(b)

**Fig.1**
a) Specimen loaded on UTM. (b) Specimen as per ASTM standard.

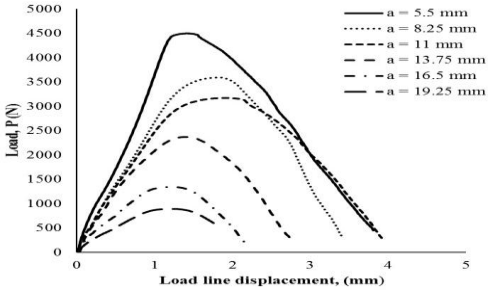


**Fig.2**
Load vs Load line displacement.

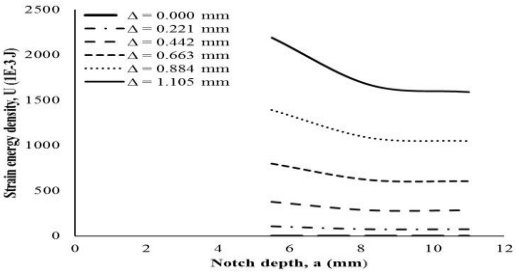


(a)

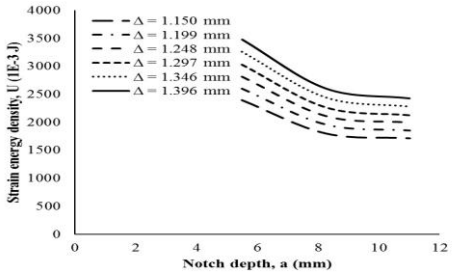


(b)

**Fig.3**
a) Variation of Strain energy density with Shallow notch depth in region 1. b) Variation of Strain energy density with Shallow Notch depth in region 2.

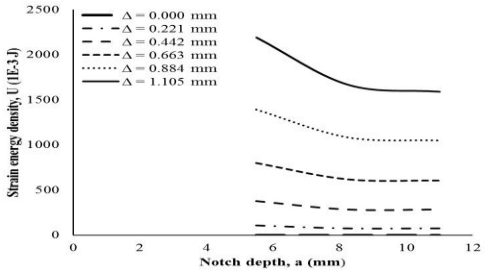


(a)

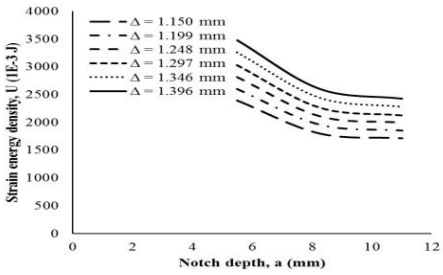


(b)

**Fig.4**
a)Variation of Strain energy density with Deep Notch depth in region 1. b) Variation of Strain energy density with Deep Notch Notch depth in region 2.

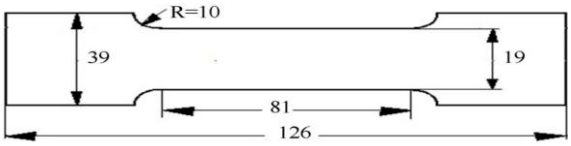


**Fig.5**
ASTM standard tensile test specimen.

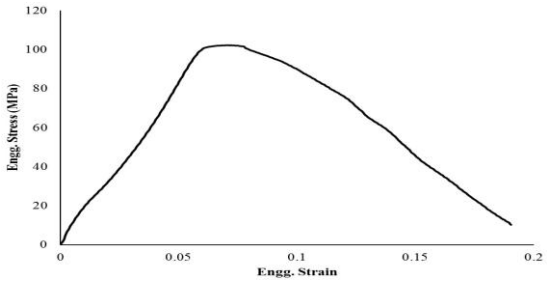


**Fig.6**
Engineering Stress – Strain curve.

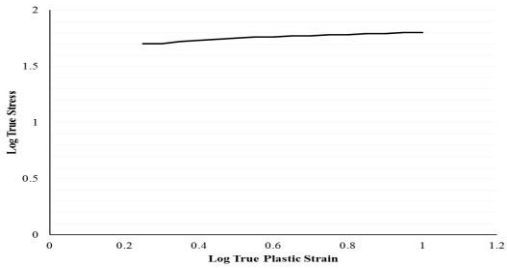


**Fig.7**
Log-Log True Stress – Plastic Strain curve.

## 3 FAILURE ASSESSMENT DIAGRAMS (FAD)

FAD's are the generally used for assessing the structural integrity of Elastic Plastic behavior of materials. The application of FAD gives the exact idea that a material is safe or not under a particular loading condition. The concept of the FAD requires the use of fracture parameters that cater for large scale plasticity. The *J*-integral is widely used for this purpose. It accounts for the possibility of fracture and plastic collapse separately. These possibilities are plotted on the axes of the FAD as $K_r$ against $L_r$. The stress intensity ratio $K_r$ is plotted on y axis and load ratio $L_r$ is plotted on the x axis. $K_r$ is equal to the square root of ratio of elastic *J* and total *J* of the material and $L_r$ is the ratio of reference stress to the yield stress. Once the diagram is generated, an assessment point is considered which may lie in the "acceptable" or "unacceptable" region of the diagram. Here the FAD was derived using strip yield model along with the concept of *J*-integral.

$$L_r = \frac{\sigma_{ref}}{\sigma_{YS}} \tag{11}$$

where

$$\sigma_{ref} = \left( P \big/ P_0 \right) \sigma_0 \tag{12}$$

The next step was to find the assessment point and plot it in this FAD. Here the parameters used were $K_r$ and $S_r$ which are the stress intensity ratio and stress ratio respectively. These parameters can assess the significance of a particular flaw in a material and can be found using;

$$K_r = \frac{K_I}{K_{mat}} \tag{13}$$

$$S_r = \frac{\sigma}{\sigma_c} \tag{14}$$

where, $K_{mat}$ is the material toughness and $\sigma_c$ is the collapse stress i.e. when the stress on the unnotched cross section reaches the ultimate stress. The corresponding collapse load can be found and the ratio of the collapse load to the applied load gives the value of $S_r$. In the FAD, the point $A$ ($S_r$, $K_r$) gave the assessment point. If the point lies inside the FAD curve, the material or component is predicted to be safe under that particular load condition. When the point falls on the curve, the corresponding load can be considered as critical load, i.e., if it falls outside the FAD curve, the structure is no longer safe.

From the above relations, it is clear that for materials with low toughness and low stress, the failure occurs in linear elastic range and is usually brittle. Similarly for materials of higher toughness and high stress, it is a case of ductile overloading and the assessment point falls towards the plastic collapse area. Between these cases, the fracture is preceded by elastic plastic deformation.

According to, Hasanaj et al., [14], the three zones in the FAD shown in Fig. 8 can be conventionally expressed as;

Zone I: $0 < L_r < 0.62L_{r,Y}$

Zone II: $0.62L_{r,Y} < L_r < 0.95L_{r,\max}$

Zone III: $0.95L_{r,\max} < L_r < L_{r,\max}$

where $L_{r,Y}$ is associated with the value of $L_r$ at yield point and $L_{r,\max}$ is the maximum value of $L_r$ .

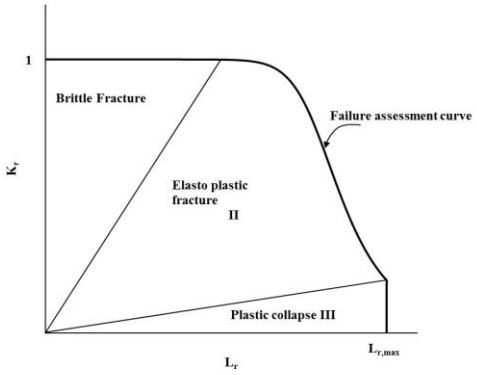


**Fig.8**
Domain Failure assessment Diagram.

## 4 RESULTS AND DISCUSSION

The notch depths considered in the experimental and analytical methods for finding *J*-integral, are categorized as shallow notches (a≤ b) and deep notches (a>b). Results showing the variation of *J*-integral versus applied load for different notch depths are presented in this section. Also, the results showing the effect of notch depth on the safe load are also explained in this section.

### *4.1 Effect of notch depth to width ratio on J-integral*

Figs. 9(a)–(f) show the comparison of analytical and experimental *J*-integral values for different notch depths, *a*, equals 5.5, 8.25, 11, 13.75, 16.5, and 19.25 *mm* respectively for the two regions. From the figures, we can see that, the *J*-integral values calculated from analytical and experimental methods, increase with increase in applied load for all the notch depths. But, for the same load, we can see that *J*-integral values increase with increase in notch depth, i.e. amount of energy released during notch expansion was decreases with increase in notch depth.

For both shallow (a≤ b) and deep (a>b) notches, i.e. Figs. 9(a)–(f), we can see that, the *J*-integral values calculated by both analytical and experimental methods are in close agreement in region 1, i.e. from zero to yield point. But in the region 2, i.e. from yielding to ultimate, the difference in the *J*-integral values calculated using analytical and experimental methods are more with increase in applied load. The *J*-integral values calculated from analytical method are deviating from the experimental values in region 2, because, in this region $J_{plastic}$ becomes dominant when load value increases and $J_{elastic}$ has less significance on applied load values.

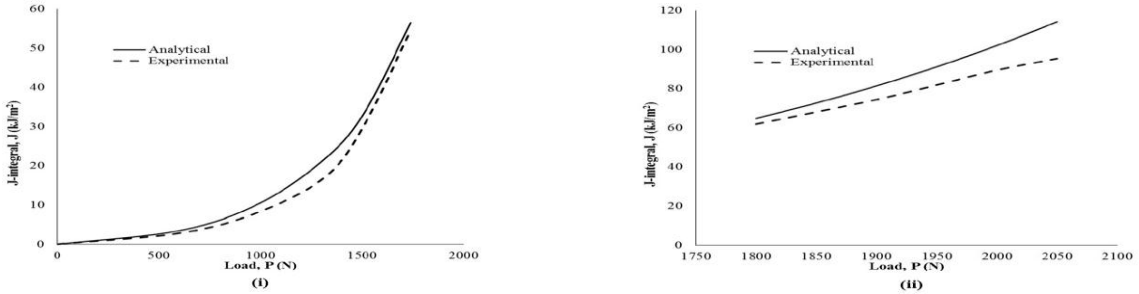


**Fig.9**
a) Variation of *J*-integral with applied for a = 5.5 *mm* (i) Region 1 and (ii) Region 2.

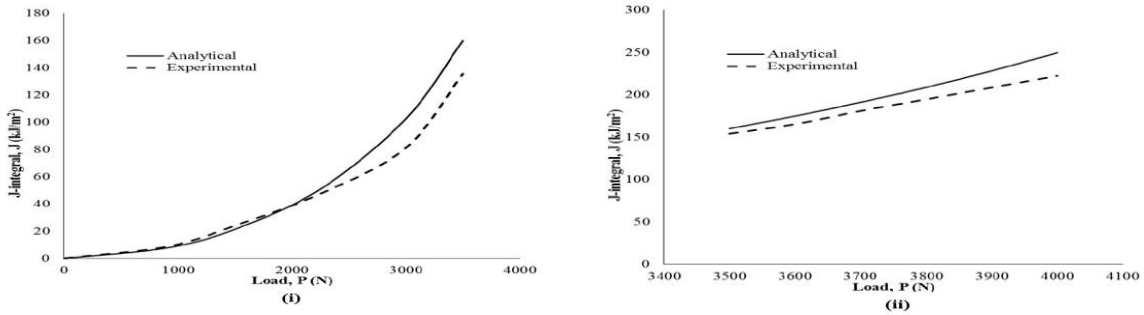


b) Variation of *J*-integral with applied for a = 8.25 *mm* (i) Region 1 and (ii) Region 2.

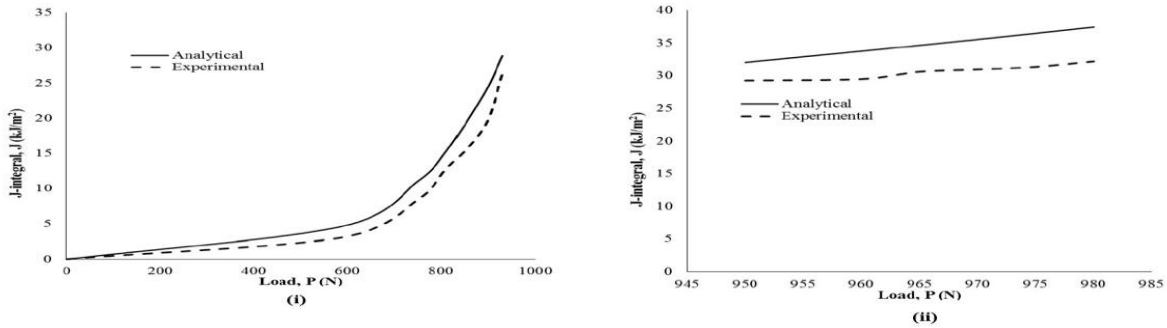


c) Variation of J-integral with applied for a = 11 mm (i) Region 1 and (ii) Region 2.

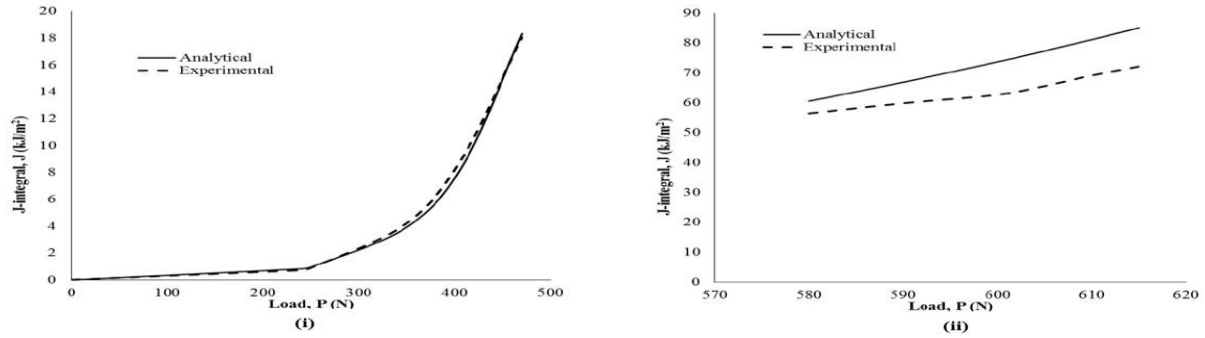


d) Variation of *J*-integral with applied for a = 13.75 *mm* (i) Region 1 and (ii) Region 2.

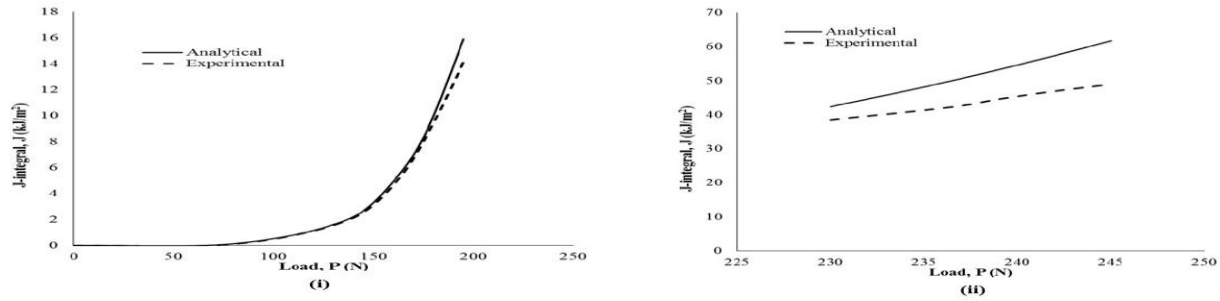


e) Variation of *J*-integral with applied for a = 16.5 *mm* (i) Region 1 and (ii) Region 2.

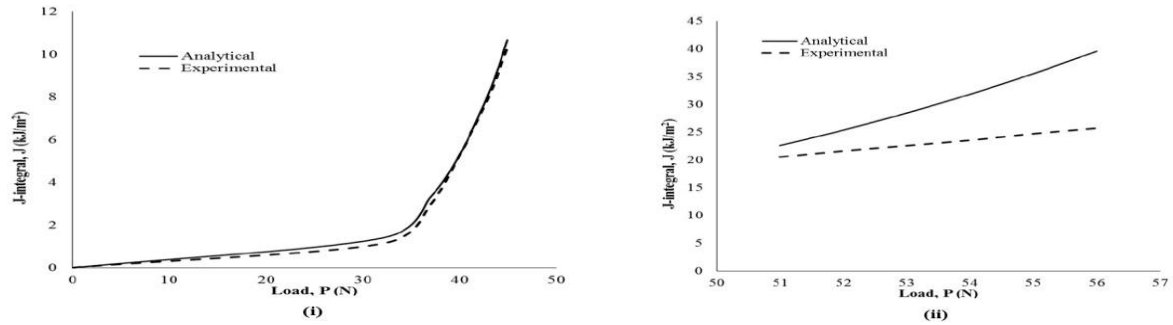


f) Variation of J-integral with applied for a = 19.25 mm (i) Region 1 and (ii) Region 2.

### *4.2 Effect of notch depth on Failure Assessment diagrams*

The values of *J* are further applied in deriving the FAD using the relations (11) – (14). The FAD along with the assessment points are plotted for each notch depth as shown below in Figs. 10(a) - (f).

The Figs. 10(a), 10(b), and 10(c) show FAD for specimens having shallow notch and 10(d), 10(e) and 10(f) show FAD for specimens having deep notch. The assessment point's fall inside the FAD curve which means that material is safe under the loading conditions. The point falling on the FAD curve is the critical load, it is the maximum load that specimen can take without failure. The points fall outside the FAD curve shows that the specimen is not safe that loading condition.

From the Figs. 10(a)–(f), the critical load for each Al 8011 specimen is given in Table 2. below. Also, by comparing Fig. 8 and Figs. 10(a)–(f), based on the position of critical point on FAD, we can say that, the failure mechanism of material Al 8011 alloy is due to elastic plastic fracture.

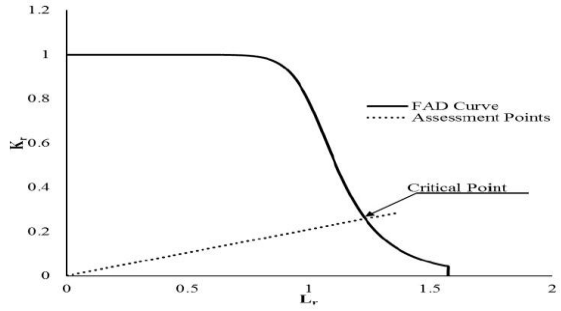


**Fig.10**
a) FAD for notch depth 5.5 mm with load - evaluation points.

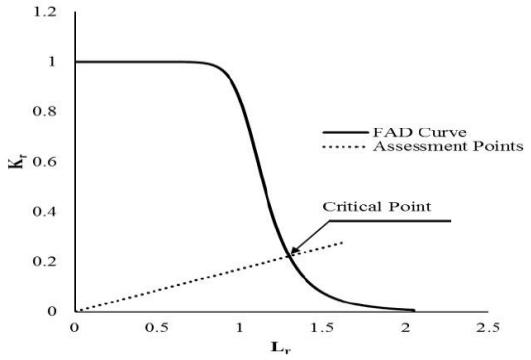


b) FAD for notch depth 8.25 mm with load – crack evaluation points.

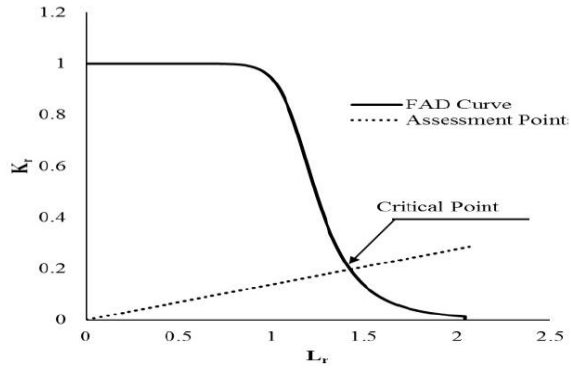


c) FAD for notch depth 11 mm with load – crack evaluation points.

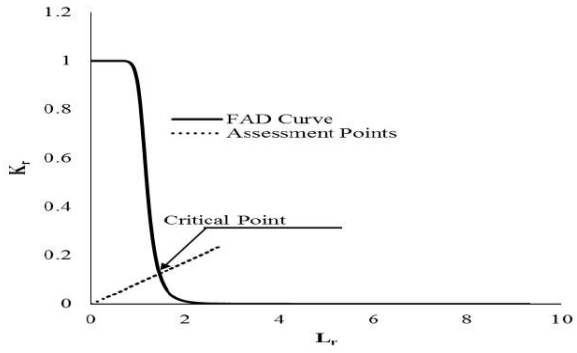


d) FAD for notch depth 13.75 mm with load – crack evaluation points.

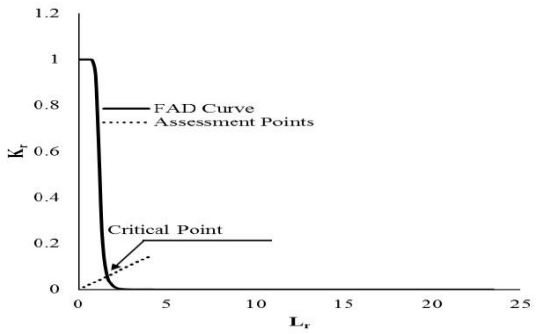


e) FAD for notch depth 16.5 mm with load - crack evaluation points.

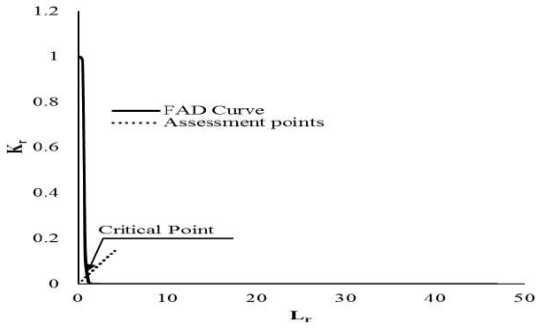


f) FAD for notch depth 19.25 mm with load – crack evaluation points.

**Table 2**
Safe load from FAD for different notch depths.

| Type of notch | Notch depth (*mm*) | Safe load from FAD (*N*) |
|---|---|---|
| Shallow | 5.5 | 4085 |
| Shallow | 8.25 | 2860 |
| Shallow | 11 | 2188 |
| Deep | 13.75 | 1227.5 |
| Deep | 16.5 | 516 |
| Deep | 19.25 | 385 |

## 5 CONCLUSIONS

The influence of notch depth to width ratios on *J*-integral and critical or safe load of specimens made from Aluminium 8011 alloy with *U*-notch under Mode I loading was studied in this paper. A set of specimens of different notch lengths as per ASTM standard was prepared and the *J*-integral was found for each specimen using analytical and experimental results. Using these *J*-integral values, failure assessment diagrams (FADs) were prepared for each specimen. The conclusions obtained from this study are:

For both shallow and deep notches, the analytical and experimental *J*-integral values are in close agreement in region 1, i.e. from zero to yield point. For both shallow and deep notches in region 2, i.e. from yielding to ultimate, the difference in analytical and experimental *J*-integral values is increasing with applied load because $J_{elastic}$ has no influence on the *J*-integral values instead $J_{plastic}$ has significant influence in *J*-integral calculation. From the FADs, the critical or safe load, i.e. the maximum load that can be applied on the material without failure, is calculated for different notch depth and it was found that, the critical load decreases with increase in notch depth. More importantly, from this we understood that the material Al 8011 alloy having notch, was failed due to elastic plastic fracture.

## REFERENCES


[1] Mohan Kumar S., Pramod R., Shashi Kumar M.E., Govindaraju H.K., 2014, Evaluation of fracture toughness and mechanical properties of Aluminum alloy 7075, T6 with Nickel coating, *Procedia Engineering* **97**: 178-185.

[2] Shih C.F., Hutchinson J.W., 1976, Fully plastic solutions and large-scale yielding estimates for plane stress crack problems, *Journal of Engineering Materials and Technology* **98**: 289-295.

[3] Vijayan V.J., Arun A., Bhowmik Sh., Abraham M.C., Ajeesh G.B., Pitchan M. Kb., 2016, Development of lightweight high-performance polymeric composites with functionalized nanotubes, *Journal of Applied Polymer Science* **133**: 43471.

[4] Kumar V., German M.D., Shih C.F., 1981, *An Engineering Approach for Elastic-Plastic Fracture Analysis*, Electric Power Research Institute, Calofornia.

[5] Shimakawa T., Asada Y., Kitagawa M. , Kodaira T., Wada Y., Asayama T., 1992, Analytical evaluation method of *J*-integral in creep-fatigue fracture for type 304 stainless steel, *Nuclear Engineering and Design* **133**: 361-367.

[6] Rice J.R., 1968, A path independent integral and the approximate analysis of strain concentration by notches and cracks, *Journal of Applied Mechanics* **35**: 379-386.

[7] Alan T., Zehnder A., Rosakis J., Krishnaswamy S., 1990, Dynamic measurement of the *j*-integral in ductile metals, *Comparison of Experimental and Numerical Techniques International Journal of Fracture* **42**: 209-230.

[8] Begley J. A., Landes J. D., 1972, The *J*- integral as a fracture criterion, *ASTM* **1972**: 1-20.

[9] Montgomery S.S. R., 1976, *J*-Integral measurements on various types of specimens in AISI 304, *Commission of the European Communities Nuclear Science and Technology* **2008**: 2-28.

[10] Aldo F., 1984, Experimental measurement of the *J*-integral engineering fracture mechanics, *Engineering Failure Analysis* **19**(4): 1105-1137.

[11] Madrazo V., Cicero S., García T., 2014, Assessment of notched structural steel components using failure assessment diagrams and the theory of critical distances, *Engineering Failure Analysis* **36**: 104-120.

[12] Tipple C., Thorwald G., 2012, Using the failure assessment diagram method with fatigue crack growth to determine leak-before-rupture, *SIMULIA Customer Conference*.

[13] Akhurst K.N., Milne I., 1984, Failure assessment diagrams and *J*-estimates: validation for an austenitic steel, *Application of Fracture Mechanics to Materials and Structures* **1984**: 401-413.

[14] Hasanaj A., Gjeta A., Kullolli M., 2014, Analyzing defects with failure assessment diagrams of gas pipelines, *World Academy of Science, Engineering and Technology International Journal of Mechanical and Mechatronics Engineering* **8**(5): 1045-1047.

[15] Marcos A., Bergant A., Yawny A., Juan E., Perez I., 2015, Failure assessment diagram in structural integrity analysis of steam generator tubes, *International Congress of Science and Technology of Metallurgy and Materials* **8**: 128-138.

[16] Xudong Q., 2013, Failure assessment diagrams for circular hollow section X- and K-joints, *International Journal of Pressure Vessels and Piping* **104**: 43-56.

[17] Matvienko Y. G., 2013, *Notch Fracture Mechanics Approaches in an Analysis of Notch-like Defects*, ECF.

[18] Matvienko Y., 2013, Safety factors in structural integrity assessment of components with defects, *International Journal of Structural Integrity* **4**(4): 457-476.

[19] Mostafa S., Elsaadany M., Younan Y.A., Hany F.A., 2014, Determination of shakedown boundary and failure-assessment-diagrams of cracked pipe bends, *Journal of Pressure Vessel Technology* **136**: 011209-1-9.

[20] Anthony H., Mikhail T., Hertele S., 2015, Failure prediction of curved wide plates using the strain- based failure assessment diagram with correction for constraint and notch radius, *Journal of Pressure Vessel Technology* **137**: 021208-1-10.

[21] Luis F.S., Parise C. R., Noel P., Dowd O'., 2015, Fully-plastic strain-based *J*-estimation scheme for circumferential surface cracks in pipes subjected to reeling, *Journal of Pressure Vessel Technology* **137**: 041204-1-8.

[22] Giorgio D., Candida P., 2010, A failure assessment diagram for components subjected to rolling contact loading, *International Journal of Fatigue* **32**(2): 256-268.

[23] Lie S.T., Li T., 2014, Failure pressure prediction of a cracked compressed natural gas (CNG) cylinder using failure assessment diagram, *Journal of Natural Gas Science and Engineering* **18**: 474-483.